Front. Chem. China 2007, 2(3): 265–269
DOI 10.1007/s11458-007-0047-z

RESEARCH ARTICLE

PEI Xianru, WANG Xiaodong, ZHANG Shunli, ZHANG Jingwei, YANG Jianjun, JIN Zhensheng

Preparation and characterization of nanotube Li-Ti-O by molten salt method

Abstract Nanotube Li-Ti-O compound with high surface (198.6 $m^2 \cdot g^{-1}$) was prepared by a method involving the treatment of nanotube $Na_2Ti_2O_5 \cdot H_2O$ in molten $LiNO_3$ and characterization by means of transmission electron microscopy (TEM), energy-dispersive spectra (EDS), X-ray diffraction (XRD), X-ray photoelectron spectroscopy (XPS), and thermogravimetry-differential thermal analysis (TG/DTG). Results show that the nanotube Li-Ti-O compound prepared by this method involves two crystal phases: spinel $Li_2Ti_2O_4$ and anatase Li_xTiO_2 ($x < 0.1$). Li^+ exhibits different Li1s binding energy in the two crystal phases. In ambient air, the Li-Ti-O compound adsorbs water easily, and the chemically adsorbed water is difficult to remove below 400°C.

Keywords nanotube $Na_2Ti_2O_5 \cdot H_2O$, nanotube Li-Ti-O compound, molten method, Li-electrode material

1 Introduction

Because of the invention of the $C/LiCoO_2$ rechargeable battery by Sony, many lithium ion battery systems with $LiCoO_x$, $LiMn_2O_4$, and $LiNiO_x$ as positive electrode materials and graphite as negative electrode material have been developed [1,2]. Recently, to avoid the shortcoming of the graphite negative electrode material (such as initial loss of the capacity, structure distortion and low specific surface area etc.) [3,4], some transition metal oxide materials such as WO_3, MoO_3 and TiO_2 were studied [3,5–7]. Among these novel materials, Li-Ti-O compounds based on TiO_2 are the most promising candidates [8,9].

Li-Ti-O compounds include stoichiometric and non-stoichiometric compounds, which have different crystal phases and can be prepared by various synthesis methods. Cava et al. [10,11] measured the structure of the reaction product of *n*-butyl-lithium with anatase TiO_2 by neutron diffraction analysis. The result showed that the host crystal cell distorts to orthorhombic when Li intercalation in TiO_2 forming $Li_{0.5}TiO_2$ (the crystal cell parameters for anatase TiO_2: a = 0.378 4 nm, b = 0.378 4 nm, c = 0.951 5 nm, for $Li_{0.5}TiO_2$: a = 0.380 8 nm, b = 0.407 6 nm, c = 0.905 3 nm), and heated over 500°C, $Li_{0.5}TiO_2$ transform to spinel $LiTi_2O_4$ (a = 0.840 3 nm), which reacts further with *n*-butyl-lithium to form $Li_2Ti_2O_4$ at room temperature, retaining its spinel structure (a = 0.837 6 nm). Wagemaker et al. [12] measured the structure of the reaction product Li_xTiO_2 of *n*-butyl-lithium with anatase TiO_2 by X-ray diffraction (XRD) method. When $x < 0.6$, anatase and lithium titanate coexist, and when $x = 0.7$, anatase completely transform to lithium titanate phase. Fattakhova et al. [13,14] obtained spinel Li-Ti-O compound by the method of hydrothermal treating TiO_2 (P25, Degussa) in 0.6 $mol \cdot L^{-1}$ LiOH solution at 120°C–200°C in autoclave. X-ray diffraction (XRD) and ^7Li magic angle spinning (MAS) nuclear magnetic resonance (NMR) results showed that the composition of the product is $Li_1 + xTi_2 - xO_4 + \delta$ ($x = 0$–1, $\delta = 0.3$ and 0.5). Rock salt $LiTiO_2$, spinel $LiTi_2O_4$ and $Li_4Ti_5O_{12}$, all belong to face-centered crystal system, but they have different crystal cell parameters. Rock salt $LiTiO_2$ is usually prepared by high temperature sintering and high temperature electrochemical synthesis method. For example, Lecerf [15] obtained $LiTiO_2$ (a = 0.414 0 nm) by treating Ti_2O_3 with Li_2O at 1 000°C. Jiang et al. [16] reported that when electrolyzing anatase TiO_2 in 700°C molten LiCl and the voltage is at 3.2 to 2.0 V, $LiTiO_2$ can be obtained. And when the voltage is below 1.8 V, $LiTi_2O_4$ can be obtained.

The specific surface area of the materials is an important parameter for controlling the rate of electrons passing in and out of the electrode. Because graphite possesses low specific surface area (3 $m^2 \cdot g^{-1}$), the Li-ion battery with graphite as the negative electrode material is not suitable for equipment which need the strong instant current [4]. Presently, the synthesis and properties of nanometer Li-Ti-O compound with high specific surface area have attracted much attention. For example, by the exchange reaction between H-titanate and LiOH solution, Zhang et al. [17] obtained one-dimension

Translated from *Chinese Journal of Inorganic Chemistry*, 2006, 22(12): 2135–2139 [译自: 无机化学学报]

PEI Xianru, WANG Xiaodong, ZHANG Shunli, ZHANG Jingwei, YANG Jianjun, JIN Zhensheng (✉)
Laboratory of Special Functional Materials, Henan University, Kaifeng 475001, China
E-mail: zhenshengjin@henu.edu.cn

spinel $Li_4Ti_5O_{12}$ products which have specific surface area of 237.6 and 126.7 $m^2 \cdot g^{-1}$, respectively, and have excellent electrochemical properties. The two Li intercalation hosts, anatase nanorod (specific surface area = 314 $m^2 \cdot g^{-1}$) [18] and H-titanate nanotube (specific surface area = 331 $m^2 \cdot g^{-1}$) [19], showed excellent potential in application. In this paper, nanotube Li-Ti-O compound was successfully prepared by treating nanotube $Na_2Ti_2O_5 \cdot H_2O$ in molten $LiNO_3$, and was characterized and analyzed.

2 Experimental

2.1 Preparation of nanotube $Na_2Ti_2O_5 \cdot H_2O$ [20]

In a (polytetrafluoroethylene) PTFE breaker, 4 g TiO_2 powder (anatase, Zhejiang Mingri Nanometer Material Company, China) was added to 150 mL of 10 $mol \cdot L^{-1}$ aqueous NaOH (Tianjin Nankai Chemical Plant, A.R.) solution and stirred. After TiO_2 was equally dispersed in the NaOH aqueous solution, the dispersion was carefully transferred to a PTFE bottle equipped with a reflux condenser placed in an oil bath. After the mixture was stirred at 120°C in PTFE bottle for 24 h, the reaction was stopped. The product dispersion was cooled to room temperature and sedimented, and then the deposit was diluted with three-time distilled water to pH = 12.5, filtered and dried.

2.2 Preparation of nanotube Li-Ti-O compound

Two grams of nanotube $Na_2Ti_2O_5 \cdot H_2O$ powder was mixed with 12 g of $LiNO_3$. The mixture was put in a crucible and heated by a sand bath at 260°C (sand bath temperature) for a definite time, and then cooled to room temperature and washed with three-time distilled water to remove superfluous $LiNO_3$(NO_3^- ions was detected by 1% diphenylamine thick H_2SO_4 solution), filtered and dried to obtain the Li-Ti-O compound. A tubular oven was used to anneal the Li-Ti-O compound at 500°C.

2.3 Characterization

Transmission electron microscopy (TEM) images were taken on a JEM-2010 electron microscope (accelerating voltage: 200 kV). Energy-dispersive spectra (EDS) were obtained on a SEM-5600 LV scanning electron microscope (SEM) equipped with energy disperse X-ray spectrometer (Britain, OXFORD Co.) (accelerating voltage: 30 kV). Specific surface area and pore size distribution are tested on an ASAP2010 surface area analyzer. XRD spectra of the samples were obtained on a Philips X' Pert Pro X-ray diffractometer (with monochromatized $Cu_{k\alpha}$ radiation, $\lambda = 1.5406$ Å, voltage 40 kV, current 40 mA). The chemical state and composition of the samples were analyzed by spectra of X-ray photoelectron spectroscopy (XPS) on an AXIS ULTRA X-ray photoelectron spectrometer (40 eV monochromatized Al Kα source, 150 W, vacuum: 7.5×10^{-11} Pa, polluted carbon (284.8 eV) as reference). The thermogravimetric (TG) curve and differential thermogravimetric (DTG) curve of the samples were determined on Seiko TG/DTA 6300 thermoanalysis system (in air, temperature programmed rate: 10°C $\cdot$ min^{-1}).

3 Results and discussion

3.1 Morphography and composition

Figure 1(A) shows the TEM image of $Na_2Ti_2O_5 \cdot H_2O$ nanotubes. Figure 1(B) and (C) show TEM images of 1.5 and 7.5 h products, respectively. After ion-exchange, nanotubular morphography remains unchanged. From Fig. 1(D) (high resolution TEM (HRTEM) image of nanotube end), the boundaries of layer-to-layer are illegible. The adjacent distance between the two layers is *ca*. 0.42 nm, shorter than that (*ca.* 0.8 nm) of the $Na_2Ti_2O_5 \cdot H_2O$ nanotubes. The inner diameter of the nanotube is *ca.* 7–8 nm, a little longer than that (Fig. 1(A)) of the $Na_2Ti_2O_5 \cdot H_2O$ nanotubes. Li^+ ions in molten $LiNO_3$ can quickly substitute for Na^+ ions in the $Na_2Ti_2O_5 \cdot H_2O$ nanotubes. EDS spectra (Fig. 2) indicate that when $t = 1.5$ h, the concentration of Na^+ ions is zero (when $t = 4.5$ h and 7.5 h, the concentrations of Na^+ ions are zero, too). According to Fig. 3, the N_2 adsorption-desorption isotherms and Barrett-Joyner-Halenda (BJH) pore size distribution curve, the Brunauer-Emmett-Teller (BET) specific surface area of the Li-Ti-O compound is 199 $m^2 \cdot g^{-1}$ and the average pore diameter is 7.8 nm (similar to the result of HRTEM).

3.2 Crystal phases

When Li^+ ions substituted for Na^+ ions, the crystal phase of the nanotubes greatly changes. Figure 4 shows XRD patterns of nanotubes $Na_2Ti_2O_5 \cdot H_2O$ and ion-exchange products. Nanotubes $Na_2Ti_2O_5 \cdot H_2O$ belong to orthorhombic [20], while Li-Na ion-exchange products contain two phases: spinel $Li_2Ti_2O_4$ [21] and anatase Li_xTiO_2 ($x < 0.1$) [10,12,22]. With the increase in reaction time, the intensities of all the peaks attributed to the two phases also increase, but the peak height ratio (R(h18°/h25°) = 0.76) for the two phases remain unchanged, indicating that the two phases exist in an equilibrium. Their empirical formula is Li_yTiO_2 ($y < 0.6$).

During discharge, batteries need to maintain a constant electrical potential between their electrodes over a range of lithium concentrations. The two-phase equilibrium system in the electrodes provides such a plateau in potential, that as only the relative phase fractions vary on charging (or discharging) of the lithium. Just as the equilibrium between liquid and vapor is maintained by a continuous exchange of particles between the two phases, a similar exchange is required to maintain equilibrium in the solid state [23]. Therefore, it is considered that as a battery material, two

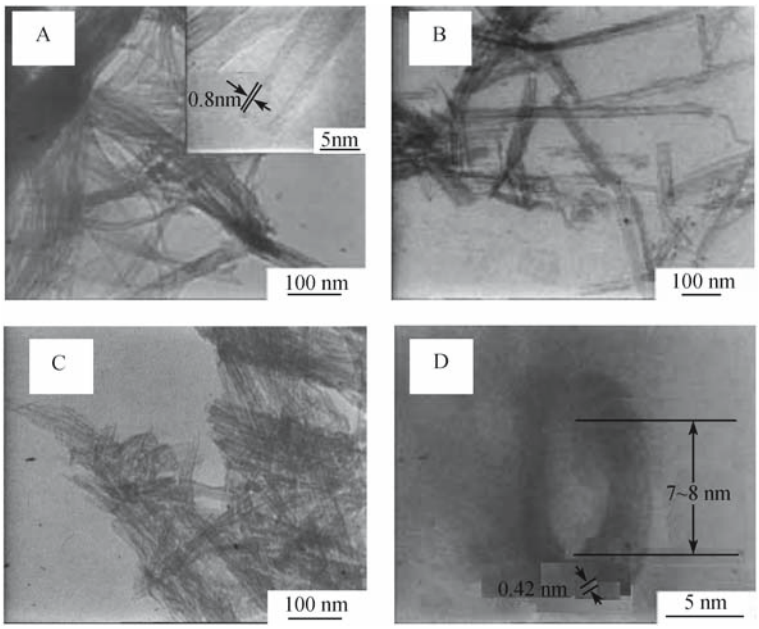

Fig. 1 TEM images of nanotube $Na_2Ti_2O_5 \cdot H_2O$ and the products (Li-Ti-O compounds) at different reaction time (A) nanotube $Na_2Ti_2O_5 \cdot H_2O$; (B) Li-Ti-O compound ($t = 1.5$ h); (C) Li-Ti-O compound ($t = 7.5$ h); (D) HRTEM image of Li-Ti-O compound ($t = 1.5$ h)

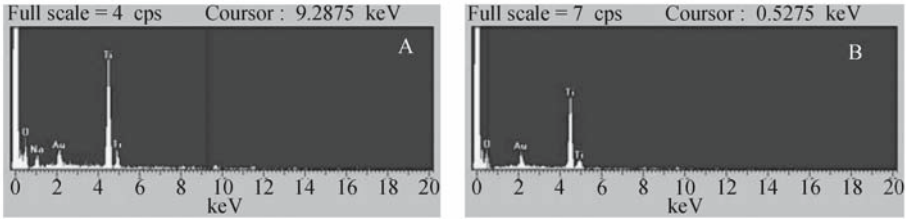

Fig. 2 EDS spectra of (A) nanotube $Na_2Ti_2O_5 \cdot H_2O$ and (B) Li-Ti-O compound ($t = 1.5$ h)

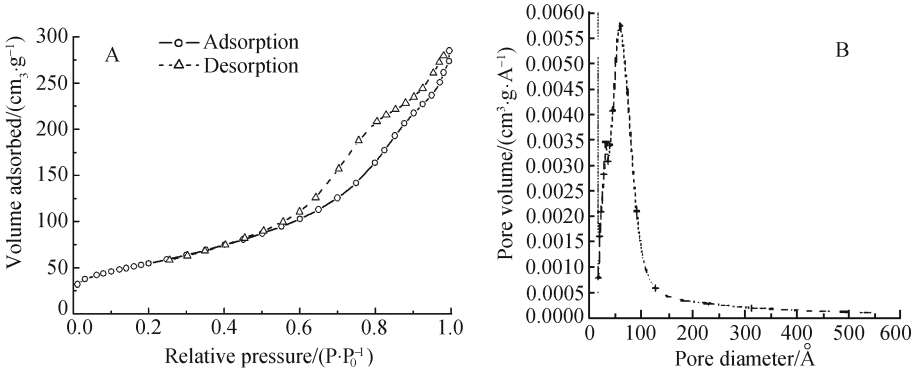

Fig. 3 Low-temperature (A) N_2 adsorption-desorption isotherms and (B) BJH pore size distribution for Li-Ti-O compound ($t = 1.5$ h)

different-phase of Li-Ti-O compounds contained in Li-Na ion-exchanging product may be an advantage.

3.3 Chemical state of Li in the product

Because the small photoelectric cross section of Li excited by X-ray results in XPS signal weakening, the scanning time for obtaining Li1s spectra was increased. Figure 5(A) shows that the deconvoluted curve includes two Li1s peaks, which E_b (binding energy) are 55.7 eV and 54.4 eV, respectively. Comparing with the spectra of LiOH [E_b(Li1s) = 55.3 eV] (Fig. 5(B)), 55.7 eV and 55.4 eV denote two chemical shift states of Li^+ ion, which are attributed to Li^+ ions in spinel and in anatase, respectively. This is consistent with the result of

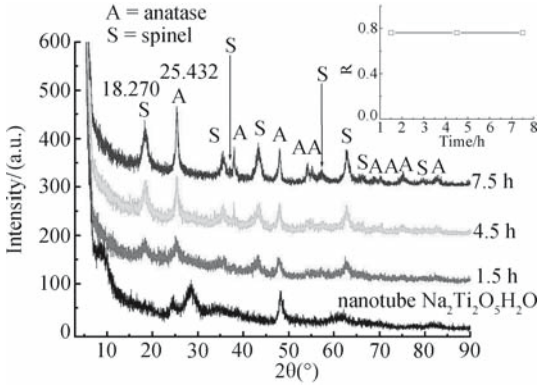

Fig. 4 XRD patterns of the nanotube $Na_2Ti_2O_5 \cdot H_2O$ and its ion-exchange products in molten $LiNO_3$ (inset: the relationship between R and t)

Wagemaker and Luca et al. [23,24]. They identified that two typical Li^+ ion chemical shift states exist in Li_xTiO_2 by MAS NMR method. Figure 5(C) shows E_b (Ti2$p_{3/2}$) = 458.9 eV, corresponds to Ti^{+4}, while E_b (O1s) = 530.0 eV and 531.9 eV (Fig. 5(D)) correspond to lattice oxygen (O^{2-}) and OH^-, respectively. Table 1 shows the relative surface atomic concentration of the reaction product of nanotube $Na_2Ti_2O_5 \cdot H_2O$ with $LiNO_3$ at 260°C. The concentration of Na is zero, consistent with the results of EDS analysis from Fig. 2.

Table 1 Relative surface atomic concentration of Li-Ti-O compound

Surface element	Li	Ti	O	Na
Atomic / %	16.1	15.9	68.0	0.0

3.4 Thermal property

Figure 6(A) shows the TG and DTG curves of Li-Na ion-exchanging product at 260°C for 1.5 h. There are two weight-loss peaks. The peak observed at around 64°C belongs to the desorption of the physically adsorbed water. The weight loss is 5.6%, indicating that the product strongly adsorbed water in air. To confirm the signification of the weight loss peak at 495°C, the product was annealed at 500°C for 2 h and then characterized by XRD. From Fig. 6(B), the positions of XRD peaks of pattern b is consistent with that of pattern a, indicating that heat-treating at 500°C does not change the crystal structure of the product. Therefore, the peak at 495°C can be attributed to the desorption of a strongly chemically adsorbed water (weight loss = 3.0%). In addition, the relative intensities of the peaks for patterns a and b changed, i.e. R (h18°/h25°) = 1.3, not 0.76, indicating that heat-treating at 500°C can increase the content of spinel in the compound.

4 Conclusions

The Li_yTiO_2 compound was prepared by molten salt method and its characteristics are as follows: first, the Li_yTiO_2 compound prepared with nanotubes $Na_2Ti_2O_5 \cdot H_2O$ as precursor maintains nanotubular structure, and its BET specific surface area is 199 $m^2 \cdot g^{-1}$; second, L_yTiO_2 involves two different crystal phases, i.e., spinel $Li_2Ti_2O_4$ phase and anatase Li_xTiO_2 phase ($x < 0.1$); third, in molten $LiNO_3$, Li-Na ion-exchanging rate is high and this exchange is complete;

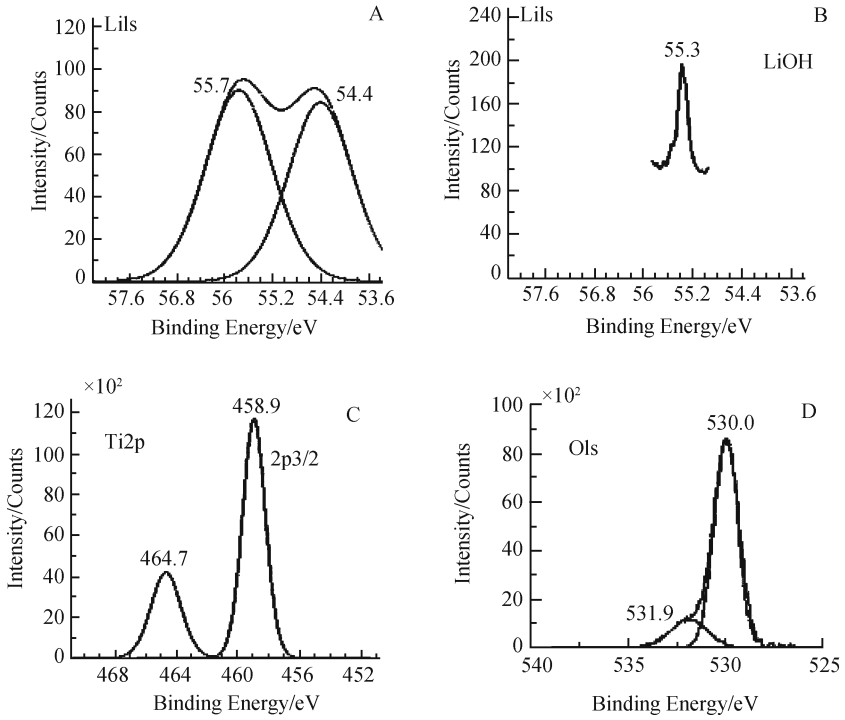

Fig. 5 XPS spectra of Li-Ti-O compound (A) Li1s spectrum; (B) Li1s spectrum of reference compound LiOH; (C) Ti2*p* spectrum; (D) O1s spectrum

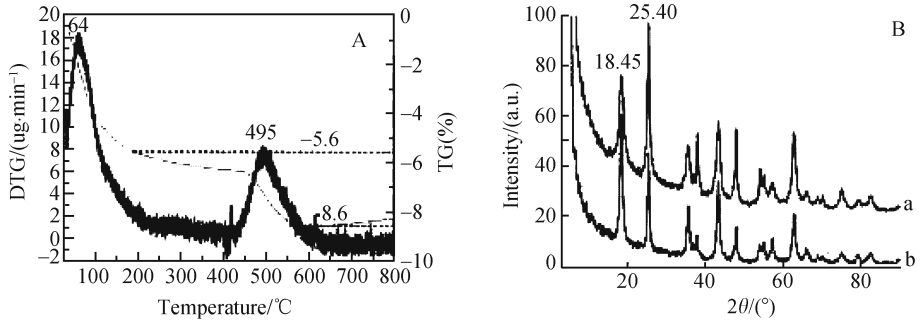

Fig. 6 (A) TG/DTG curve of Li-Ti-O compound and (B) its XRD patterns

finally, heat-treating at 500°C can increase the content of spinel in the compound.

Acknowledgements We thank Gao Xinyong, Li Jian and Zhang Yudong for HRTEM, XPS, DG/DTG experiments.

References

1. Nagaura T, Tozawa K. Lithium ion rechargeable battery. Prog Batteries Solar Cells, 1990, 9: 209
2. Tarascon J M, Armand M. Issues and challenges facing rechargeable lithium batteries. Nature, 2001, 414: 359–367
3. Natarajan C, Setoguchi K, Nogami G. Preparation of a nanocrystalline titanium dioxide negative electrode for the rechargeable lithium ion battery. Electrochim Acta, 1998, 43: 3371–3374
4. Duncan G R. New Scientist. London: New Science Publications, March 5, 2005
5. Abrham K M. Directions in secondary lithium battery research and development. Electrochim Acta, 1993, 38: 1233–1248
6. Auborn J J, Barbero Y L. Lithium intercalation cells without metallic lithium. J Electrochem Soc, 1987, 134: 638–641
7. Huang S Y, Kavan L, Exnar I, Grätzel M. Rocking chair lithium battery based on nanocrystalline TiO_2 (Anatase). J Electrochem Soc, 1995, 142: L142
8. Ohzku T, Takehara Z, Yoshizawa S. Nonaqueous lithium/titanium dioxide cell. Electrochim Acta, 1979, 24: 219–222
9. Bomino F, Busani L, Lazzani M, Manstretta M, Rivolta B, Scrosati B. Anatase as a cathode material in lithium-organic electrolyte rechargeable batteries. J Power Source, 1981, 6: 261–270
10. Cava R J, Murphy DW, Zahurak S, Santoro A, Roth R S. The crystal structures of the lithium-inserted metal oxides $Li_{0.5}TiO_2$ anatase, $LiTi_2O_4$ spinel, and $Li_2Ti_2O_4$. J Solid State Chem, 1984, 53(1): 64–75
11. Murphy DW, Cava R J, Zahurak S M, Santoro A. Ternary Li_xTiO_2 phases from insertion reactions. Solid State Ionics, 1983, 9–10: 413–417
12. Wagemaker M, van de Krol R, Kentgens A P M, van Well A A, Mulder F M. Two phase morphology limits lithium diffusion in TiO_2 (Anatase): A ^{7}Li MAS NMR study. J Am Chem Soc, 2001, 123: 11454–11461
13. Fattakhova D, Petrykin V, Brus J, Kostlánová T, Dědeček Jiri and Krtil P. Solvothermal synthesis and electrochemical behavior of nanocrystalline cubic Li–Ti–O oxides with cationic disorder. Solid State Ionics, 2005, 176(23–24): 1877–1885
14. Fattakhova D, Krtil P. Electrochemical Activity of Hydrothermally synthesized Li-Ti-O cubic oxides toward Li insertion. J Electrochem Soc, 2002, 149: A1224–A1229
15. Lecerf A. Sur Quelques Propriétés Chimiques des Oxydes TiO et Ti_2O_3. Ann Chim, 1962, 7: 513–535 (in French)
16. Jiang K, Hu X H, Sun H J, Wang D H, Jin X B, Ren Y Y, Chen G Z. Electrochemical synthesis of $LiTiO_2$ and $LiTi_2O_4$ in molten LiCl. Chem Mater, 2004, 16(2): 4324–4329
17. Li J R, Tang Z L, Zhang Z T. Controllable formation and electrochemical properties of one-dimensional nanostructured spinel $Li_4Ti_5O_{12}$. Electrochem Commu, 2005, 7: 894–899
18. Gao X P, Zhu H Y, Pan G L, Ye S H, Lan Y, Wu F, Song D Y. Preparation and electrochemical characterization of anatase nanorods for lithium-inserting electrode material. J Phys Chem B, 2004, 108: 2868–2872
19. Li J R, Tang Z L, Zhang Z T. H-titanate nanotube: A novel lithium intercalation host with large capacity and high rate capability. Electrochem Commun, 2005, 7: 62–67
20. Yang J J, Jin Z S, Wang X D, Li W, Zhang J W, Zhang S L, Guo X Y, Zhang Z J. Study on composition, structure and formation process of nanotube $Na_2Ti_2O_4(OH)_2$. Dalton Trans, 2003, 20: 3898–3901
21. JCPDS 77–1389
22. JCPDS 84–1286
23. Wagemaker M, Kentgens A P M, Mulder F M. Equilibrium lithium transport between nanocrystalline phases in intercalated TiO_2 anatase. Nature, 2002, 418: 397–399
24. Luca V, Hanley T L, Roberts N. K, Howe R F. NMR and X-ray absorption study of lithium intercalation in micro- and nanocrystalline anatase. Chem Mater, 1999, 11(8): 2089−2102